Cell. Mol. Biol. (ISSN: 1165-158X)

Journal Homepage: www.cellmolbiol.org

Cellular and Molecular Biology

Original Article

Pan-cancer analysis of TMEM45A and exploration of its prognostic value and mechanism in gastric cancer

Qixin Xie, Tao Guo, Hong Deng, Changjun Yu, Changyi Fang*

Department of General Surgery, The First Affiliated Hospital of Anhui Medical University, Hefei, China

Article Info

Article history:

Received: March 14, 2024
Accepted: April 09, 2024
Published: July 31, 2024

Use your device to scan and read the article online

Abstract

Cancer is a major category of diseases that need to be addressed urgently, bringing a huge burden to the world. Gastric cancer (GC) is a frequent malignant tumor of the digestive system with the highest incidence and mortality rate among all tumors. The purpose of this study was to explore the mechanism of action of TMEM45A in pan-cancer and gastric cancer. First, GEO and TCGA database were employed to analyze the expression of TMEM45A in GC patients. Then, we determined the association between TMEM45A expression and survival of GC patients using the Kaplan-Meier Plotter database and TCGA database and verified the accuracy of TMEM45A in predicting prognosis. Next, we analyzed the effect of CTHRC expression on TIICs in GC tissues. A prognostic model was constructed using immunomodulatory genes associated with TMEM45A. The specificity and accuracy of the model were verified. TMEM45A expression was markedly higher in GC tissue than in normal tissue. GC patients with TMEM45A overexpression had a poor prognosis. The AUC value of 5-year survival on the ROC curve was 0.705, indicating that TMEM45A is a reliable prognostic factor and can be used as a clinicopathological indicator alone to predict patient prognosis. Three high-risk immunomodulatory genes (CXCR4 and TGFB1) and one low-risk immunomodulatory gene (PDCD1) were obtained using both univariate and multivariate COX methods. These three immunomodulatory molecules were used to construct prognostic models. GC patients with TMEM45A overexpression have a poor prognosis and are associated with immune cell infiltration. Hence, TMEM45A is a fairly reliable independent prognostic marker.

Keywords: TMEM45A, Pan-cancer, GC, Prognosis, Model.

1. Introduction

In every country in the world, cancer is the leading cause of death and a significant barrier to increasing life expectancy. According to WHO estimates, in 2019, cancer was the first or second leading cause of death before age 70 in 112 out of 183 countries, and third or fourth in another 23 countries. The rising incidence of cancer is the leading cause of death as well [1]. Currently, the enthusiasm in the medical community for fighting cancer is high, but with that comes constant attention. Therefore, more and more researchers are looking for cancer-related markers to determine the prognosis of cancer patients.

Gastric cancer (GC) is a malignancy of the digestive system. It ranks fourth among all cancers and is one of the leading causes of death worldwide [2]. GC is a global health concern, with at least 1 million new cases and more than 700,000 deaths in 2020, placing a heavy burden on the global economy. The incidence of GC has a strong geographical correlation, with higher incidence in East Asia, Central and South America and Eastern Europe and lower incidence in North America and Africa, probably due to differences in dietary habits [3, 4]. There are numerous risk factors that affect the occurrence of GC, including *Helicobacter pylori* infection, age, genetic risk factors, intake of nitrate, alcohol, pickling, high salt, fermentation, improper food storage, etc. [5-9]. Although radiological examinations, serological blood tests and endoscopic screening of the high-risk population have slightly reduced the rate of GC, the prognosis of GC patients is still poor, with a high mortality rate [10-12]. Therefore, there is a need to explore accurate prognostic indicators and prognostic models to recognize patients at high risk of death and to provide timely and appropriate treatment strategies.

TMEM proteins are a class of transmembrane family proteins whose members have transmembrane structures in the cell membrane and are involved in the regulation of various cellular functions and signaling pathways. TMEM proteins are classified into three main groups according to their functions: transporter proteins, receptor proteins and signaling proteins. The TMEM protein is quite rich in functions and plays a role in many diseases. For example, in asthma, the activation of TMEM16A by inflammatory mediators makes airway smooth muscle (ASM) more sensitive to cholinergic stimulation, and this sensitivity is an important factor in the development of airway hyperreactivity [13,14]. In head and neck squamous cell carcinoma

* Corresponding author.
E-mail address: chyfrank@163.com (C. Fang).
Doi: http://dx.doi.org/10.14715/cmb/2024.70.7.32

(HNSCC), combination therapy with TMEM16A and PD-L1 inhibitors improves survival in patients with HNSCC, especially those resistant to epidermal growth factor receptor (EGFR) inhibitors [15]. TMEM196 inhibits the Wnt signaling pathway and suppresses β-cyclin promoter transcription to strongly inhibit lung cancer metastasis and progression in vivo and in vitro [16]. TMEM163 has been reported to be a zinc efflux transporter protein with physiologically relevant interactions with solute carrier 30 (SLC30), and their heterodimerization may contribute to the functional diversity of zinc efflux in specific tissues or cell types, which has led to the association of TMEM163 directly or indirectly with a wide range of human diseases, such as Parkinson's disease, type IV mucolipidosis and diabetes [17-19]. TMEM175 has been shown to be a genetic risk factor for Parkinson's disease (PD), mediating lysosomal H[+] leakage by acting as a proton-activated, proton-selective channel on the lysosomal membrane (LyPAP). Deficiency of TMEM175 leads to lysosomal over-acidification, and impaired protein hydrolysis, and promotes the aggregation of α-synuclein in vivo, which results in the loss of lysosomal normal function [20].

TMEM45A is also a transmembrane protein, and to date, little is known about this protein, particularly its expression in cancer and its mechanism of action. In head and neck squamous cell carcinoma (HNSCC) and renal cell carcinoma (RCC), knockdown of TMEM45A reduces cell proliferation and cellular response to cisplatin, which may be related to the inhibition of DNA damage repair and activation of the UPR pathway [21, 22]. It has been shown that, in vivo, high expression of TMEM45A promotes epidermal keratinization and accumulates in the trans-Golgi/trans-Golgi network of keratinocytes, does not reach the lysosomal compartments, and is finally localized mainly in the granular layer of the epidermis, which is a result indicating a strong correlation between the expression of TMEM45A and epidermal keratinization [23, 24]. Variations in the TMEM45A gene have been reported and proposed as the genetic basis for isolated congenital globus pallidus, with the possible mechanism being the promotion of up-regulation of extracellular matrix components and fibrosis in corneal stroma and epithelial cells [25]. In human ovarian cancer, inhibition of TMEM45A expression can inhibit the proliferation of cancer cells, induce the arrest of the cell cycle, and reduce the cell's ability to invade [26]. TMEM45A is overexpressed in ccRCC, is associated with poorer survival and acts as a tumor promoter and, therefore, may be a potential prognostic marker and therapeutic targetM45A [27].

To date, the relationship between TMEM45A and gastric cancer has not been studied. This study aimed to further investigate the relationships amongTMEM45A expression, the prognosis of GC patients and immune cell infiltration, and prognostic outcome in GC patients, which can provide new ideas for GC immunotherapy.

2. Materials and Methods

2.1. Cell Lines and Cell Cultures

Human gastric cancer cell lines including HGC-27 and MKN-45 as well as normal gastric epithelial cells GES-1 were purchased from Priscilla. HGC-27, MKN-45 andGES-1 were cultured in RPMI-1640 medium. In addition, 10% fetal bovine serum (Gibco) and penicillin-streptomycin (Gibco) were added to the medium. The cells were grown in an incubator with temperature of 37°C and humidity of 5% CO_2.

2.2. Cell transfection

According to the experimental grouping, the cells were inoculated in 6-well culture plates with 10^5~10^6 cells per well, 3 replicate wells were designed for each group, and the cells were cultured in complete medium (1640+10% FBS+1% double antibody) overnight and then grouped for treatment. The groups were HGC-27 control group, HGC-27 sh-NC group, HGC-27 si-TMEM45A group, MKN-45 control group, MKN-45 sh-NC group and MKN-45 si-TMEM45A group for culture. Cell transfection was performed 24 h after cell seeding plates with cell densities of 30%-50%. Cells were collected for RNA extraction 24 years after transfection.

2.3. Western Blot Analysis

Cells were collected and fully lysed with IP cell lysate (containing PMSF) on ice. Cell lysates were centrifuged in an ultracentrifuge at 4°C, 12,000 rpm for 10 min and protein concentration was measured using the BCA Protein Assay Kit (Beyotime). Protein samples were mixed with sampling buffer, boiled in boiling water for 5 min, rapidly cooled on ice, and resolved by polyacrylamide gel electrophoresis. After electrophoresis, proteins were electrophoretically transferred to polyvinylidene difluoride (PVDF; Roche) membranes using a semi-dry blotter (Bio-Rad). After transfer, the membranes were incubated in phosphate-buffered saline (PBS) containing 5% skimmed milk and 0.1% Tween-20 for 2 hours at room temperature. Membranes were incubated with primary antibodies against human C-MYC (Affinity, AF6054), B-catenin (Affinity, BF8016), and GAPDH (Proteintech, 60004-1-Ig) overnight at 4°C, and then with horseradish enzyme-labeled goat-anti-rabbit IgG (Nakasugi Jinqiao, ZB-2301) at room temperature. 2301) and goat anti-mouse IgG (Zhongsui Jinqiao, ZB-2305) at room temperature. After washing with PBS, the immunoreactive bands were observed using Chemistar High-sig ECL Western Blotting Substrate.

2.4. RNA extraction and Quantitative Real Time-Polymerase Chain Reaction (qRT-PCR)

Extract total RNA from cells using TRIzol reagent according to the manufacturer's instructions. The cDNA was then prepared using the reverse transcription kit Hifair II 1st Strand cDNA Synthesis Kit (manufacturer: YEASEN). Primer Premier 5.0 and Beacon Designer 7.8 software were used for the design of quantitative PCR primers, which were then synthesized by General Biological Co. The primers used in this research were as follows: F-5'-ACAACTTTGGTATCGTGGAAGG and R-5'-GCCATCACGCCACAGTTTC for GAPDH. F-5'-GGCTCCTGGCAAAAGGTCA and R-5'-CTGCGTAGTTGTGCTGATGT for c-Myc. F-5'-CATGCCCTCCCTGGAACCTT and R-5'-CTCCCCAGCCATGCCAGTTA for TMEM45A. F-5'-GCCTGTTCCCCTGAGGGTATT and CCATCAAATCAGCTTGAGTAGCCA for β-catenin. SYBR Green qPCR Mix (manufacturer: Biosharp) was carried out for the qRT-PCR.

2.5. Cell counting kit 8 (CCK 8) determination

According to the experimental grouping, HGC-27 and

MKN-45 cells were inoculated into 96-well culture plates, the number of cells per well was 3000, and 3 replicate wells were designed for each group. After 24 h of incubation, 10 μL of CCK-8 reagent was added to each well of the 96-well plate, and the cells were incubated at 37°C in a 5% humidified CO_2 incubator for 2 h. The OD value at 450 nm was measured on an enzyme counter.

2.6. Transwell Assay

1000 cells were inoculated into the upper chamber of the transwell of a 24-well plate, 100 μL of serum-free medium was added to the upper chamber, and 600 μL of medium containing 20% serum was added to the lower chamber and incubated for 24 h. The cells in the lower layer of the chamber were fixed with methanol for 15 min, stained with 0.1% crystal violet for 20 min, washed twice with PBS, and photographed under the microscope. The cells in the lower layer of the chamber were fixed with methanol for 15 minutes, stained with 0.1% crystal violet for 20 minutes, washed twice with PBS, and photographed under the microscope.

2.7. Flow Cytometry

According to the experimental grouping, the cells were inoculated in 6-well culture plates with 10^5~10^6 cells per well, 3 replicate wells were designed for each group, and the cells were cultured in complete medium (1640+10% FBS+1% double antibody) overnight and then grouped for treatment. The groups were HGC-27 control group, HGC-27 sh-NC group, HGC-27 si-TMEM45A group, MKN-45 control group, MKN-45 sh-NC group and MKN-45 si-TMEM45A group for culture. Cell transfection was performed 24 h after cell seeding plates with cell densities of 30%-50%. Cell staining was performed after 48 hours of incubation at 37°C in a 5% CO2 incubator. The final assay was performed in a flow cytometer.

2.8. Wound-healing scratch assay

The cells were cultured in 6-well plates in a medium containing 10% fetal bovine serum and penicillin-streptomycin and grew to 100% in a carbon dioxide incubator at 37°C and 5% humidified. The wound is then manually scratched in the cell monolayer with the plastic tip. The wound was photographed with an optical microscope system at 0h and 24 h.

2.9. Acquisition of pan-cancer expression data

The gene expression and clinical data were downloaded from GDC Data Portal website (https://cancergenome.nih.gov/). GDC integrates and classifiers data to provide unified cancer genome data, including 68 primary sites and 33,549 cases. It contains data from several large-scale cancer genome research projects, including TCGA and OCG. The gene expression data were standardized. The analysis used data from 463 patients with stomach cancer. Patients with missing and duplicate clinical information were deleted, The data set GSE54129 and GSE19826 was obtained from Gene Expression Omnibus (https://www.ncbi.nlm.nih.gov/geo/).

2.10. Sparkle website analysis

Sparkle is a newly developed, feature-rich and comprehensive database (https://grswsci.top/analyze). Sparkle can perform not only single-gene analysis but also multi-gene analysis. We used the Sparkle website to analyze the association between TMEM45A expression and tumor immune subtypes.

2.11. TIMER database analysis

TIMER utilizes RNA-Seq data to determine the infiltration of six types of immune cells in tumor tissue, which are B cell, CD4 T cell, CD8 T cell, neutrophil, macrophage and dendritic cell [28, 29]. TIMER can also analyze the correlation of genomic and transcriptomic changes between tumor immune infiltrated populations and cancers, providing insights into tumor-immune interactions. TIMER was employed to analyze the expression of TMEM45A in pan-cancer. The online site was also be used to determine whether TMEM45A copy number variation (CNV) can affect immune cell infiltration.

2.12. GEPIA database analysis

GEPIA database integrates the datasets of GTEx normal tissue and TCGA cancer and employs bioinformatics technology to reveal cancer subtypes, genes, alleles or oncogenic factors, so as to further explore novel cancer markers and targets. It can allow us more simple and fast data mining, and dynamic analysis of gene expression profiles. In this experiment, c-MYC and β-catenin were analyzed based on the following conditions: |Log2FC|Cutoff> 2, p-value Cutoff<0.05.

2.13. TNMplot database analysis

TNMplot builds an integrated database using transcriptome-level datasets and creates a web platform to mine this database by comparing normal, tumor, and metastatic data for all genes in real time. The main function of TNMplot is to compare the expression of genes in normal, tumor and metastatic tissues. We used the TNMplot database to compare the differential expression of TMEM45A in normal and gastric tissues.

2.14. Kaplan-Meier (KM) plotter database analysis

By integrating clinical prognostic values and gene expression data, the Kaplan Meier Plotter database was utilized for the study, discovery and validation of survival-associated molecular markers via Meta-analysis. KM plotter was employed to analyze the relationship between TMEM45A expression and prognostic outcomes in GC patients, including disease-specific survival (DSS), overall survival (OS), progression-free interval (PFI) and disease-free survival (DFI).

2.15. TISIDB database analysis

TISIDB (http://cis.hku.hk/TISIDB/) is a database of tumor-immune interactions[30] . In TISIDB, we can easily look for the immune relationships between specific genes and the tumorigenesis environment. TISIDB database was utilized to obtain the correlations among TMEM45A, lymphocytes and immunostimulator genes.

2.16. ROC curve drawing and independent prognostic analysis

To verify the accuracy of TMEM45A in predicting prognosis, the survival ROC R software package v4.1.0 was applied to draw ROC curves for estimating 1-, 3- and 5-year survival. The higher the AUC value, the higher the specificity and sensitivity. Survival R software package

was employed for univariate and multivariate independent prognostic analyses to investigate whether TMEM45A is a prognostic indicator for GC patients.

2.17. CCLE database analysis

Cancer Cell Line Encyclopedia (https://portals.broadinstitute.org/ccle) consisted of 26 kinds of cancer cell lines. We retrieved the cell line data for all cancers from this website and used Perl software to extract the cell line data for GC and the expression levels of all genes. It was used in limma, ggplot2, ggpubr and ggExtra packages in R software to obtain genes with co-expression relationship with TMEM45A through co-expression analysis. The filtering conditions set for correlation test were: correlation coefficient corFilter >0.5, correlation test p-value <0.001. In R software, the enrichPlot package, ClusterProfiler package, GGplot2 package, org.hs.eg. db package and Pathview package were employed to perform GO and KEGG enrichment analyses of TMEM45A co-expressed genes.

2.18. Establishment of immunoregulatory gene prognostic model

We identified survival-associated genes from all immunoregulatory genes and then constructed immunoregulatory risk models by multifactorial Cox regression analysis. Then, the patient's risk value was calculated based on the following equation: Riskscore=coef(gene1)*expr(gene1)+coef(gene2)*expr(gene2)+coef(gene3)*expr(gene3)+coef(gene4)*expr(gene4)+... coef(genen)*expr(gene n). Patients were categorized into low- and high-risk groups based on their median risk values. To verify whether there was a survival difference between the high- and low-risk groups, survival curves of TCGA GC patients were plotted using the survival kits. We performed the following analyses to measure the accuracy of the model. Risk curves were used to determine whether there was a difference in mortality between patients in the high- and low-risk groups. To determine whether the prognostic model could be employed as a clinical feature alone to predict the prognosis of patients, univariate and multivariate independent prognostic analyses were conducted using the Survival R software package. To verify the prediction accuracy of clinical factors and the survival model, survival ROC R software package was employed to draw multi-index receiver operating characteristic curve (ROC). The higher the AUC value, the higher the specificity and sensitivity. In order to further verify the model's accuracy, the calibration line diagram and calibration curve were also constructed.

2.19. Statistical analysis

The correlations among TMEM45A expression and immunomodulatory genes were assessed using Spearman's correlation coefficient. The hazard ratio (HR) and 95% confidence interval (CI) were evaluated using both univariate and multivariate Cox proportional hazards regression models. All statistical tests were operated with R software v4.1.0. P<0.05 was regarded as statistically significant.

3. Results

3.1. Expression of TMEM45A in GC pan-cancer

The mRNA expression of TMEM45A was remarkably elevated in most cancer tissues compared to normal tissue, as shown by TIMER online biomarker analysis (Figure 1A). Figure 1B shows the expression of TMEM45A in some cancers. Previous studies have classified 30 types of non-blood cancers into 6 immune subtypes according to the immune expression characteristics of tumors, namely C1 - wound healing type, C2 - IFN-γ Dominant type, C3 - inflammatory type, C4 - Lymphocyte Depleted type, C5 - Immunologically Quiet type, and C6 - TGF-β Dominant type. Immune subtypes are associated with survival in cancer patients. The C3 subtype has the best prognosis, and C1 and C2 patients have a worse prognosis. Patients with the C4 and C6 subtypes of cancer had the worst prognosis [31]. We used the Sparkle website to analyze the relationship between TMEM45A expression and immune subtypes. The results showed that the expression level of TMEM45A was high in C1, C2 and C6, while the expression level of TMEM45A was low in C3 (Figure 1C). These results suggest that high expression of TMEM45A may be associated with poorer prognosis in pancarcinoma. Somatic copy number variation is the main source of genetic changes in human cancer and plays an important role in cancer progression [32]. We used the Sparkle website to analyze the relationship between TMEM45A and copy number variation. The results showed that TMEM45A had significant copy number variation in pancarcinoma. And it also analyzes the TMEM45A that exists in part of cancer copy number variations, these cancers including KIRC, ESCA, TGCT, PCPG, UCS and UVM (Figure 2A). Figure 2B showed that the copy number variation level of TMEM45A was positively correlated with the expression

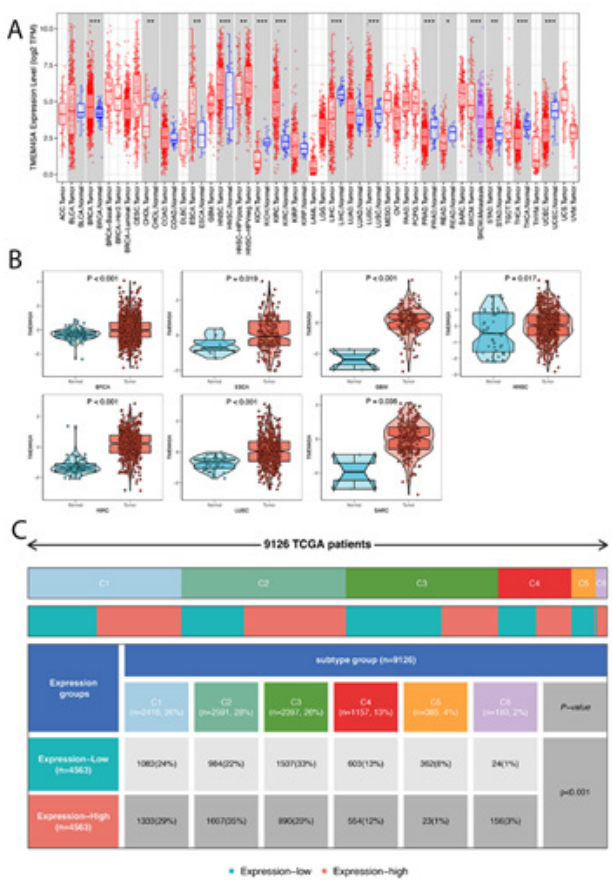

Fig. 1. Expression of TMEM45A in GC pan-cancer (A) The mRNA expression of TMEM45A was remarkably elevated in most cancer tissues compared to normal tissue, as shown by TIMER online biomarker analysis. (B) shows the expression of TMEM45A in some cancers. (C) showed that the expression level of TMEM45A was high in C1,C2 and C6, while the expression level of TMEM45A was low in C3.

level of TMEM45A in some cancers. We also used kruskal algorithm and wilcox test respectively to analyze the relationship between TMEM45A and stage. We use kruskal algorithm to find that, in the part of cancer in different stages TMEM45A expression quantity is different, these cancers including READ, KICH, KIRC, TGCT, BRCA, BLCA and SKCM (Figure 3A). We also used wilcox test analysis to show that TMEM45A is expressed differently in stageI-II and stageIII-IV in some cancers (Figure 3B).

3.2. TMEM45A has a high prognostic value in cancer

To investigate the prognostic value of TMEM45A, we performed a number of prognostic analyses, including overall survival (OS), disease-specific survival (DSS), progression-free interval (PFI) and disease-free survival (DFI). Cox regression model analysis demonstrated that high expression of TMEM45A was a risk factor for OS in patients with the according 11 tumor types (Figure 4A), including BLCA, UCEC, PAAD, KIRP, KIRC, LIHC, OV, KICH, THCA, LGG, CHOL (Figure 4B). Further research revealed that TMEM45A expression was also markedly associated with DSS (Figure 5A) in an array of carcinoma categories, such as BLCA, UCEC, PAAD, KIRP, KIRC, LIHC, OV, KICH, THCA, LGG, CHOL (Figure 5B). Cox regression model analysis demonstrated that high expression of TMEM45A was a risk factor for DFI in patients with the according 3 tumor types (Figure 6A). Cox regression model analysis demonstrated that high expression of TMEM45A was a risk factor for PFI in patients with the according 8tumor types (Figure 6B).

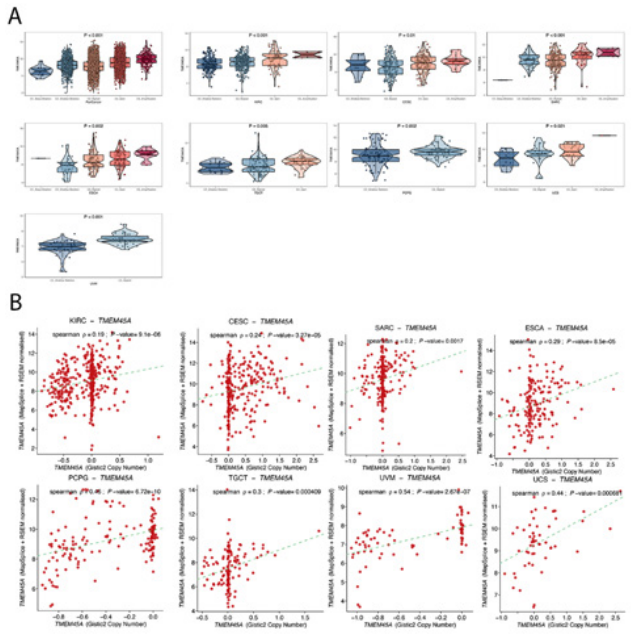

Fig. 2. TMEM45A was associated with copy number variation. (A) Copy number variation of TMEM45A was found in KIRC, ESCA, TGCT, PCPG, UCS and UVM. (B) The expression level of TMEM45A was positively correlated with copy number variation in KIRC, ESCA, TGCT, PCPG, UCS and UVM.

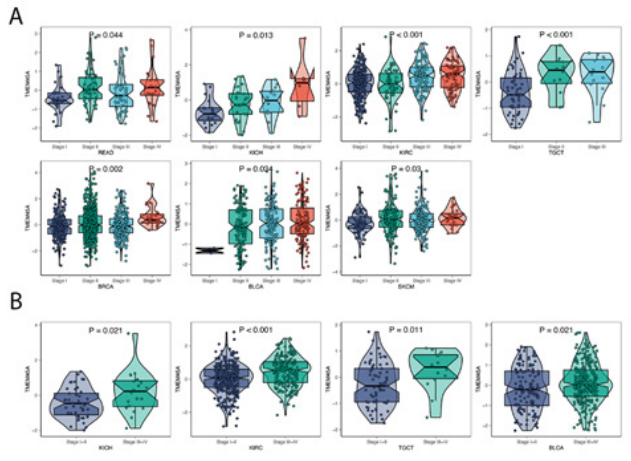

Fig. 3. The expression of TMEM45A is related to stage.(A) By kruskal algorithm, the expression of TMEM45A in READ, KICH, KIRC, TGCT, BRCA, BLCA and SKCM is correlated with tage.(B) We also used wilcox test analysis to show that TMEM45A is expressed differently in stageI-II and stageIII-IV in some cancers.

3.3. Effect of TMEM45A expression on chemotherapy drug sensitivity

We used the Sparkle website to predict the susceptibility of TMEM45A to different chemotherapy agents. The Sparkle website's chemotherapy drug analysis includes data from four databases: CTRP, GDSC1, PRISM and GDSC2. In CTRP, the higher the expression of TME-

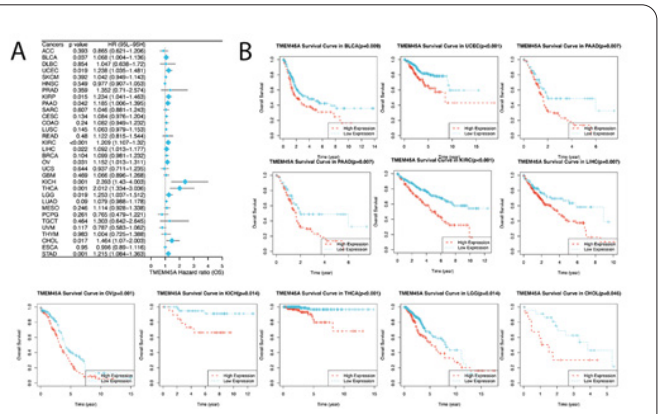

Fig. 4. Univariate COX regression analysis of TMEM45A with OS inpan-cancer. (A) Cox regression model analysis demonstrated that high expression of TMEM45A was a risk factor for OS in patients with the according 11 tumor types (B)Showed a detailed prognostic analysis of TMEM45A in 11 tumors.

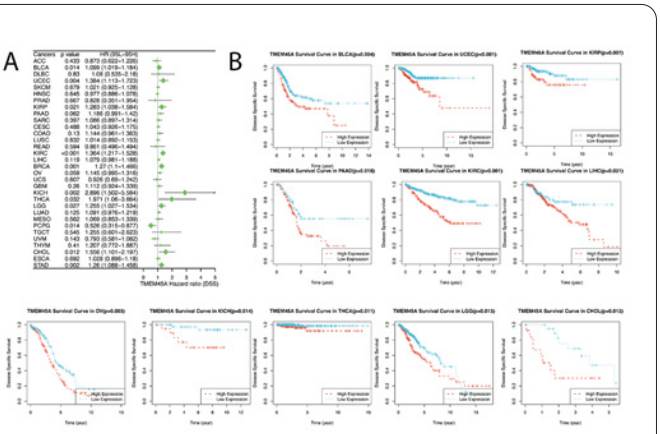

Fig. 5. Univariate COX regression analysis of TMEM45A with DSS in pan-cancer (A) Cox regression model analysis demonstrated that high expression of TMEM45A was a risk factor for DSS in patients with the according 11 tumor types (B) Showed a detailed prognostic analysis of TMEM45A in 11 tumors.

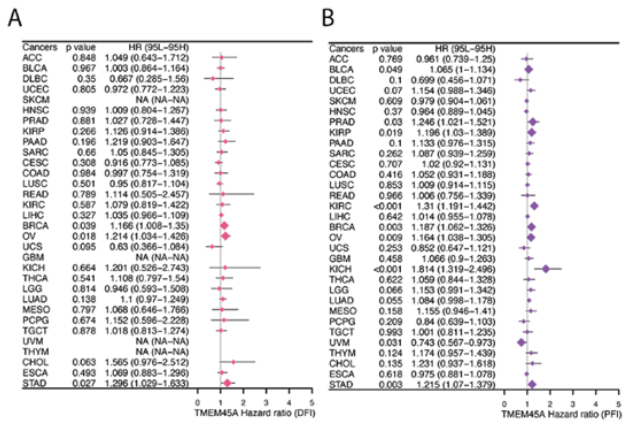

Fig. 6. Univariate COX regression analysis of TMEM45A with DFI and PFI in pan-cancer.

M45A, the higher the sensitivity of tumor cell lines to CAL-101 and vemurafenib, and the lower the sensitivity of tumor cell lines to Compound 23 citrate and austocystin D (Figure 7A). In GDSC1, the higher the expression of TMEM45A, the higher the sensitivity of the tumor cell line to Docetaxel and the lower the sensitivity of the tumor cell line to TPCA-1(Figure 7B). In PRISM, the higher the expression of TMEM45A, the higher the sensitivity of the tumor cell line to monensin and the lower the sensitivity of the tumor cell line to ciclesonide (Figure 7C). The higher the expression of TMEM45A in GDSC2, the lower the sensitivity of the tumor cell line to Vorinostat (Figure 7D).

3.4. Potential function analysis of TMEM45A in human cancers

To further understand the effect of TMEM45A on the prognosis of tumor patients, we conducted pan-oncogene set enrichment analysis (GSEA). The resulting map showed significant enrichment in cell proliferation pathways, including the MAPK signaling pathway, TGF−beta signaling pathway, and Wnt signaling pathway. in addition, the co-expressed gene set was also present in Pathways in cancer, further demonstrating the carcinogenicity of TMEM45A (Figure 8).

3.5. Expression of TMEM45A in GC

To assess the differential expression of TMEM45A in GC patients, we downloaded gene expression data from the TCGA database and performed differential analysis and paired difference analysis of TMEM45A expression in all GC patients using R software. The data indicated that the mRNA expression of TMEM45A was markedly higher in GC tissue than in normal tissue (Figure 9A). And we further validated the expression of TMEM45A using GEO datasets GSE54129 and GSE19826. The results further showed that the mRNA expression level of TMEM45A was significantly up-regulated in patients with gastric cancer (Figure 9B, 8C). We also used TNMplot database to detect the expression of TMEM45A. Similarly, TMEM45A was up-regulated in gastric cancer tissues (Figure 9D). We also verified the expression of TMEM45A in cells. The results showed that compared with normal gastric epithelial cells GES-1, the expression of TMEM45A in gastric cancer cell lines HGC-27 and MKN-45 was significantly increased (Figure 9E).

3.6. Poor prognosis for stomach cancer patients with TMEM45A overexpression

To analyze the correlation between TMEM45A expression and GC prognosis, we divided all stomach cancer patients into high- and low-expression groups. We analyzed the relationship of TMEM45A overexpression with DSS, OS, PFIand DFI in GC patients using the Kaplan Meier plotter database, and the findings demonstrated that TMEM45A overexpression was associated with shorter DSS, OS, PFIand DFI (Figure 10A). We validated the sensitivity and specificity of TMEM45A to predict prognosis by plotting ROC curves. The results showed that the AUC values were 0.601, 0.639 and 0.705 for estimating 1-, 3- and

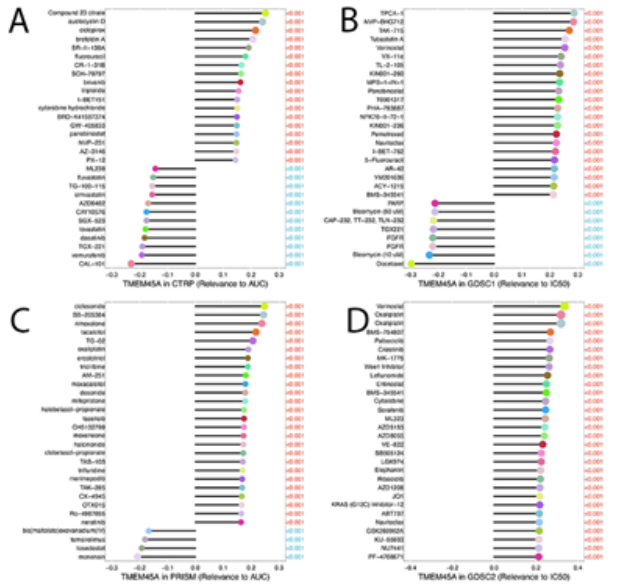

Fig. 7. Effect of TMEM45A expression on chemotherapy drug sensitivity. (A) CTRP was used to analyze the correlation between TMEM45A expression and AUC. The negative correlation means that the higher the expression of TMEM45A, the more sensitive the tumor cell line is to the drug. The length of the line and the size of the ball represent the size of the correlation coefficient. (B) GDSC1 was used to analyze the correlation between TMEM45A expression and IC50. (C) PRISM was used to analyze the correlation between TMEM45A expression and drug AUC. (D) GDSC2 was used to analyze the correlation between TMEM45A expression and IC50.

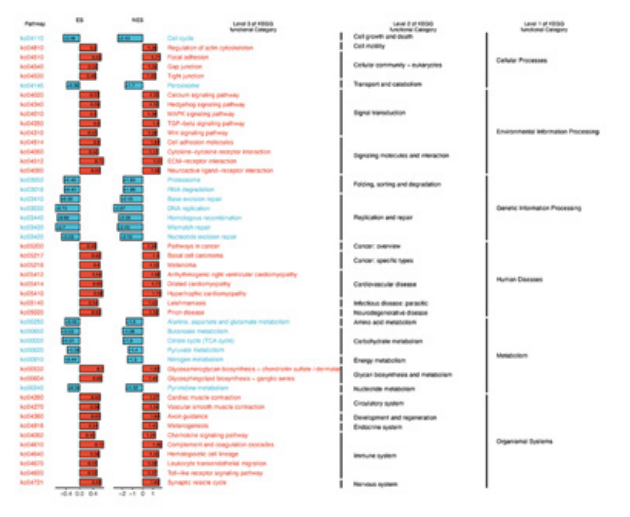

Fig. 8. Potential function analysis of TMEM45A in human cancers.

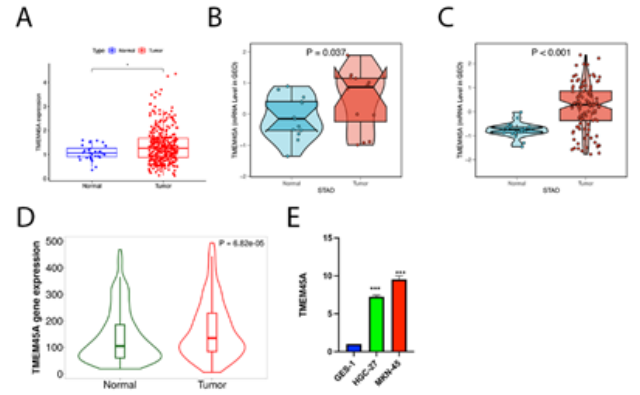

Fig. 9. The expression of TMEM45A was analyzed by using GEO, TCGA, and UALCAN databases. (A-D) The expression level of TMEM45A was significantly higher in GC patients compared with normal tissues in TCGA database and GEO database. (E)Compared with GES-1, the expression of TMEM45A was significantly increased in HGC-27 and MKN-45. * P < 0.05, **P < 0.01, ***P < 0.001. (R software v4.1.0).

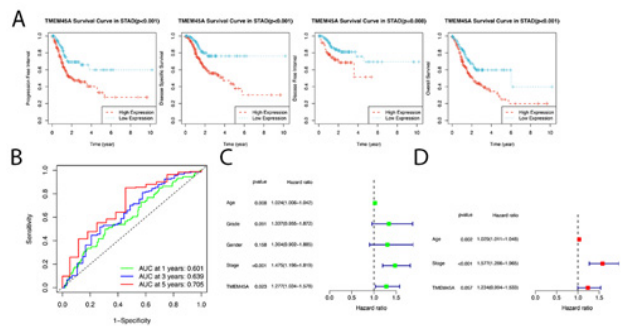

Fig. 10. TMEM45A is a reliable prognostic biomarker in GC. (A) The prognosis of gastric cancer patients with high expression of TMEM45A is poor. (B) The results of the ROC curve showed that the AUC values were 0.601, 0.639 and 0.705, respectively, which were used to estimate 1, 3 and 5-year survival rates. (C,D) Univariate and multifactorial independent prognostic analyses were conducted to determine whether TMEM45A could be used as an independent clinicopathological factor to determine the prognosis of patients. * P < 0.05, **P < 0.01, ***P < 0.001.(R software v4.1.0).

5-year survival, respectively (Figure 10B). To determine whether TMEM45A could be used as a clinical characteristic to predict patient prognosis, we performed one-way and multi-way independent prognostic analyses. The results showed HR of 1.277 (95%CI 1.034-1.578, P=0.023) and 1.234 (95%CI, 0.994-1.533, P=0.057) for the risk scores in both univariate and multifactor Cox regression analyzes (Figure 10C, 9D). Therefore, TMEM45A is a fairly reliable prognostic indicator.

3.7. The promoter region of TMEM45A has a good prognosis after methylation

We download DNA methylation data from TCGA database and use R software for data analysis. The results showed that there were 9 methylation sites in the promoter region of TMEM45A (Figure 11A). We found that the expression level of TMEM45A decreased with the increase of methylation level in the promoter region of TMEM45A (Figure 11B). More importantly, we found that the level of methylation site cg10770076 increased and the expression level of TMEM45A decreased (Figure 11C). Patients with high levels of the methylation site cg10770076 had a better prognosis (Figure 11D). This result further verified the correlation between TMEM45A expression and patient prognosis.

3.8. Correlation analysis of TMEM45A expression with immune cell infiltration

The tumor microenvironment is mainly composed of tumor cells, surrounding immune and inflammatory cells, cancer-associated fibroblasts (CAFs) and nearby interstitial tissues. The lymphocytes that infiltrate around the tumor are called tumor infiltrating lymphocytes (TILS), and these lymphocytes help the tumor cells achieve immune escape and promote the progression of the malignant tumor. CAFs can release stromal cell derived factors and pro-angiogenic factors to promote tumor cell growth and tumor blood vessel formation.In this paper, we used the Sparkle website to analyze the relationship between TMEM45A expression and the tumor immune microenvironment. The results showed that the expression of TMEM45A was positively correlated with TMEscore (Figure 12). Previous studies have shown that TMEscore can act as a prognostic factor for gastric cancer and can be used to predict the efficacy of immune checkpoint inhibitors [33]. We also found that the expression of TMEM45A is strongly correlated with macrophages and CAFs. Immune cell correlation heat maps showed that major TMEM45A was more correlated with M2 macrophages (Figure 12). M2 macrophages have a strong tumor promotion effect. Figure 13A shows the relationship between TILs abundance and TMEM45A expression in different human cancers. Figure 13B shows six tumor-infiltrating lymphocytes with the strongest correlation with TMEM45A expression, including Mast, MDSC, Monocyte, Neutrophil, pDC and Neutrophil. These cells can play an immunosuppressive role,

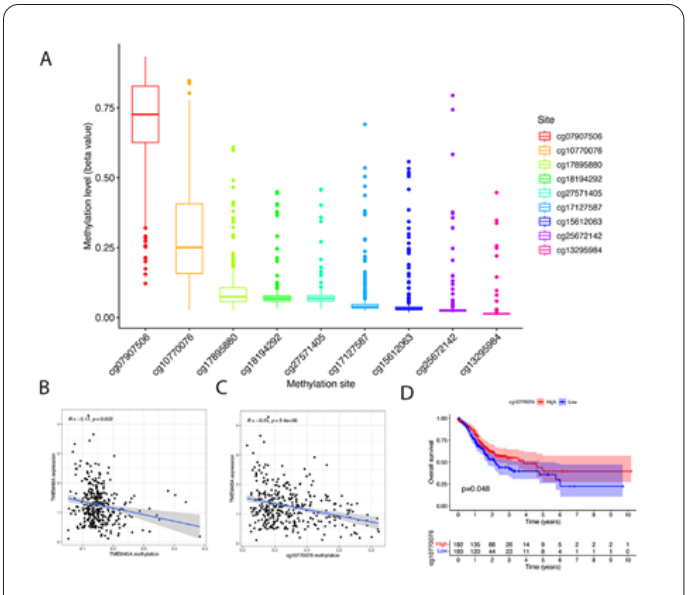

Fig. 11. The promoter region of TMEM45A has a good prognosis after methylation (A) Methylation sites in the TMEM45A promoter region. (B) The methylation level of TMEM45A was negatively correlated with the expression level of TMEM45A. (C) The level of cg10770076 methylation site of TMEM45A was negatively correlated with the expression level of TMEM45A. (D) The prognosis of patients with hypermethylation site cg10770076 was better.

enable tumor cells to escape the surveillance and killing of immune cells, promote the immune escape of tumor cells, and promote the progression of tumors. These results suggest a poor prognosis for gastric cancer patients with TMEM45A overexpression.

3.9. The high expression of TMEM45A promotes the progression of gastric cancer

We used si-RNA to interfere with the expression of TMEM45A in HGC-29 and MKN-45 gastric cancer cell lines. The results showed that compared with the control group, the expression of TMEM45A in HGC-29 and MKN-45 was significantly decreased (Figure 14A). CCK-8 experiment showed that the proliferation ability of MKN-45 decreased after the downregulation of TMEM45A (Figure 14B). Transwell Assay showed that the migration capacity of HGC-29 and MKN-45 decreased significantly after downregulation of TMEM45A (Figure 14C). Flow Cytometry showed that down-regulation of TMEM45A could induce apoptosis (Figure 14D). Cell cycle experiments showed that the number of cells in G2 phase increased significantly after the downregulation of TMEM45A (Figure 14E). Wound-healing scratch assay showed that the migration ability of cells decreased after downregulation of TMEM45A (Figure 14F).

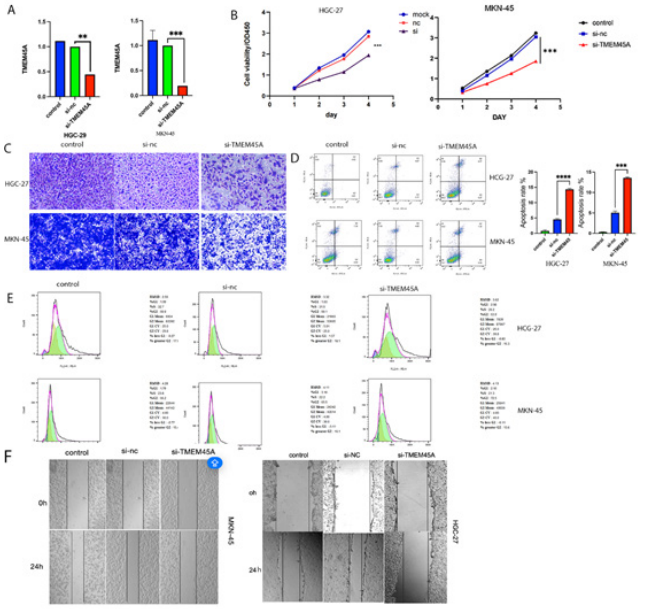

Fig. 14. The high expression of TMEM45A promotes the progression of gastric cancer. (A) shows the successful knockdown of TMEM45 in HGC-27 and MKN-45. (B,C) The ability of cell migration and proliferation decreased after TMEM45A knockdown. (D) TMEM45A knockdown promotes apoptosis. (E) After TMEM45A knockdown, the number of cells in G2 phase increased significantly.

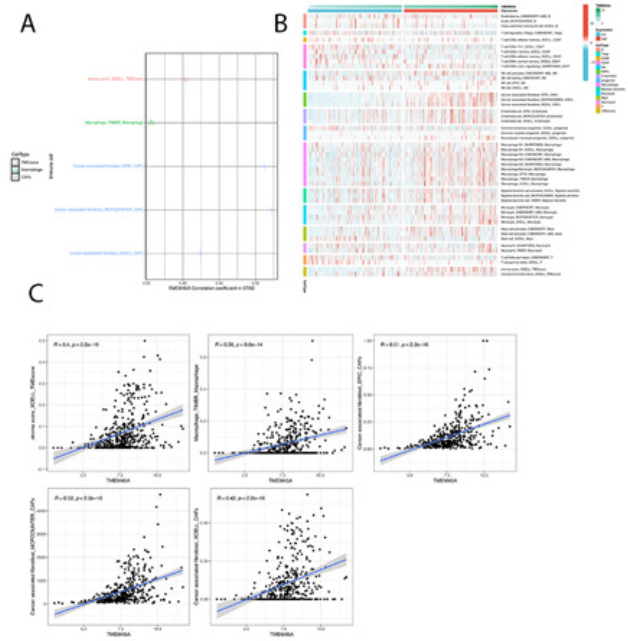

Fig. 12. Correlation between TMEM45A and tumor microenvironment. (A,C) TMEM45 is positively correlated with CAFs, TMEscore and macrophages in the microenvironment. (B) TMEM45 expressed the difference in microenvironment composition.

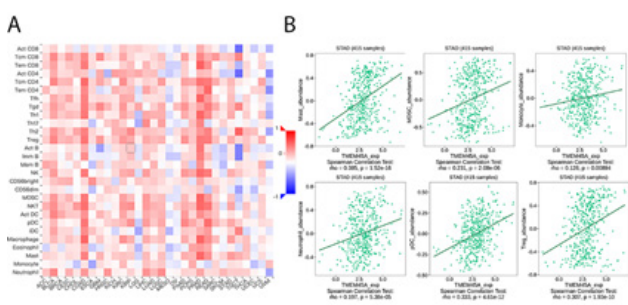

Fig. 13. The TISIDB database was used to obtain Spearman correlations of TMEM45A with various lymphocytes. (A) The effects of TMEM45A on lymphocyte infiltration in a variety of cancers. (B) The six cell types that were most associated with TMEM45A expression.

3.10. TMEM45A activates the Wnt/β-catenin signaling pathway

We used CCLE database to obtain data on GC cell lines. Genes co-expressed with TMEM45A were obtained by co-expression method. The results showed that 388 genes were co-expressed with TMEM45A. TMEM45A co-expressed genes were also selected for functional analysis and GSEA enrichment analysis. To further elucidate the role of TMEM45A in GC, GSEA was performed on the H-TMEM45A and L-TMEM45A groups, which were divided by the median level of TMEM45A expression. H-TMEM45A is abundant in WnT SIGNALING PATHWAY (Figure 15A). We further experimentally verified whether TMEM45A can activate the WnT SIGNALING PATHWAY. We used the GEPIA database to verify the expression of c-MYC and β-catenin in gastric cancer. The results showed that the mRNA expression levels of c-MYC and β-catenin were significantly increased in gastric cancer (Figure 15B). The mRNA expression levels of c-MYC and β-catenin in MKN-45 and HGC-27 were significantly increased compared with GES-1 (Figure 15C). In addition, we detected the expression of c-MYC and β-catenin in HGC-29 and MKN-45 after TMEM45A knockdown at gene level and protein level, respectively. The results showed that both c-MYC and β-catenin were significantly reduced in gene and protein levels (Figure 15D-14F).

3.11. Construction of immunoregulatory gene prognostic model

We assessed the relationship between two immune

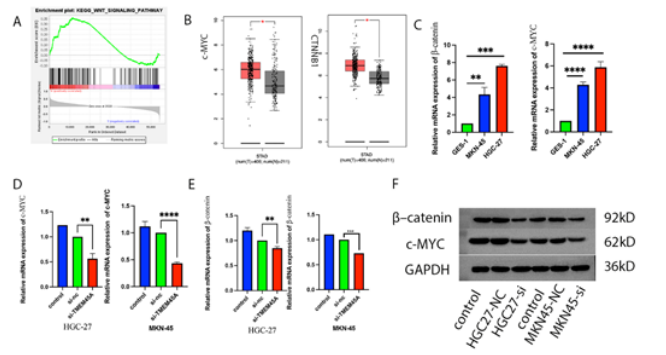

Fig. 15. TMEM45A activates the Wnt/β-catenin signaling pathway. (A) KEGG analysis of co-expression gene of TMEM45A. (B) c-MYC and β-catenin are highly expressed in gastric cancer. (C) The mRNA expression levels of c-MYC and β-catenin in MKN-45 and HGC-27 were significantly increased compared with GES-1. (D-F) After TMEM45A knockdown, the expression of c-MYC and β-catenin in mRNA level and protein level were down-regulated.

modulators and TMEM45A expression using the TISIDB database, which included 24 immunoinhibitors and 45 immunostimulators. The result shows the relationship between immunostimulators and TMEM45A expression in different human cancers, of which 30 immunostimulators were related to TMEM45A expression. To further predict GC prognosis, a prognostic model was established using immunomodulatory molecules associated with TMEM45A. Six prognostic immunoregulatory molecules were screened by univariate COX from 30 immunoregulatory molecules, including one low-risk immunoregulatory molecule (HR<1) and 5 high-risk immunomodulatory molecules (HR>1) (Figure 16A). In addition, by multivariate Cox analysis, three immunoregulatory molecules were screened out from the above 6 prognostic immunoregulatory molecules, including one low-risk immunoregulatory molecule (PDCD1) and two high-risk immunoregulatory molecules (CXCR4 and TGFB1) (Figure 16B). These three immunomodulatory molecules were subsequently used to establish optimal prognostic risk models. All GC patients were assigned to low- and high-risk groups according to the model formula. The survival analysis revealed that GC patients in high-risk group had a worse prognosis (Figure 16C). Risk curves and scatter plots were used to demonstrate the risk scores and survival status of patients, suggesting that high-risk patients had higher mortality (Figure 16D). Heatmap of four immunomodulatory molecules showed that CXCR4 and TGFB1 expression was upregulated in high-risk group, while PDCD1 was overexpressed in low-risk group (Figure 16E). To further validate the model's accuracy, the predictive value was evaluated. The specificity and sensitivity of the prognostic models were assessed by calculating the AOC values. The results showed that the survival model combined with other clinicopathological parameters had a good prediction effect. The AUC value was 0.747, suggesting that the prediction model is very reliable (Figure 16F). Univariate and multivariate Cox regression analyses were employed to determine whether the four immunoregulatory molecular prognostic models could serve as independent predictors of GC. In univariate and multivariate Cox regression analyses, the HR values of risk score were 2.215 (95%CI 1.701−2.885, P<0.001) and 2.227(95%CI 1.710−2.902, P<0.001) (Figure 16H, 15I). Therefore, it can be seen from the above results that the survival model of four immunomodulatory molecules may serve as an independent predictor.

4. Discussion

Cancer has always plagued humanity and placed a heavy burden on the global economy. About 18 million people are diagnosed with cancer each year, and about 9 million people die from it [34]. Therefore, cancer prevention, screening and treatment efforts are imperative. Pan-cancer analyses of different tumors provide comprehensive insights into tumor biology and cancer molecular phenotypes, which can help identify genomic changes that may play an important role and also point the way to finding biomarkers for targeted therapies [35].

GC is one of the most frequent cancers around the world, with a higher incidence in men than in women, mostly occurring between 60 and 80 years old. It is highly malignant and has a high mortality rate. Although the incidence and mortality of GC have decreased recently owing to the emphasis on early screening and improvement of treatment techniques, GC still poses a serious medical burden, especially in East Asia [36]. TNM staging is the most important clinical indicator for prognostic prediction and treatment. However, some studies have reported that TNM staging cannot be fully used to predict the prognostic outcomes of cancer patients [37-39]. Due to the tumor heterogeneity, individual differentiation is considerably great, and even the prognosis of patients with the same stage may be different. Therefore, it is necessary to discover new molecular markers or models for exploring the molecular mechanisms of GC, so as to more accurately

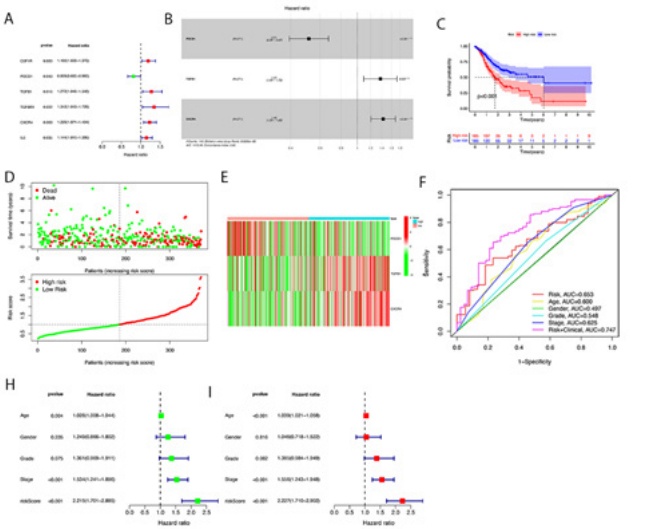

Fig. 16. Prognostic value of a survival model consisting of four immunomodulatory genes. (A, B) Screening of immunomodulatory genes in prognostic model. (C) Survival curves of GC patients in different groups. (D) Low to high-risk curves for all GC patients. The band tabulates the survival status of all GC patients. The blue dots represent survival, and the red dots represent death. The number of deaths was significantly higher in GC patients with higher risk. (E) Heat map showing that CXCR4 and TGFB1 were upregulated in the high-risk group. PDCD1 was upregulated in the low-risk group. (F) AUC values and ROC curves for risk scores and clinical factors. (H) Results of univariate Cox regression analysis of the risk model. (I) Results of multivariate Cox regression analysis of the risk model.

judge the prognosis of GC patients and better develop clinical treatment strategies.

TIICs in the tumor microenvironment have been shown to play a key role in tumor occurrence and influence the clinical outcomes of cancer patients. TIICs are highly heterogeneous and plastic, which can inhibit cancer or support tumor growth [40]. It has been reported that the distribution and morphology of TIICs are varied in different stages of GC, thereby affecting the progression and prognosis of GC patients [41, 42]. Many studies have shown that tumor-related genes can be used as molecular markers to reflect the level of immune cell infiltration in tumors. For example, CALD1 expression may influence the prognosis of GC patients by regulating GC immune cells [43]. In GC patients, LCP1 can regulate the interactions among immune cells and is significantly and positively correlated with the invasiveness and poor prognosis of GC patients [44]. The differentiation of TIICs in GC may predict the prognosis of GC patients, and become key influential factors for GC treatment [45].

In this study, we first demonstrated the expression of TMEM45A in pancarcinoma, and we found that TMEM45A is upregulated in most cancers. We found that the expression level of TMEM45A was related to stage and CNVs. We also found that TMEM45A has good prognostic value in pancarcinoma. We demonstrated the overexpression of TMEM45A in GC using multiple databases and elucidated that TMEM45A may be a reliable prognostic marker in GC patients. Additionally, our analysis indicated that TMEM45A expression in GC could affect the level of immune cell infiltration and different immune regulation. This study further demonstrated the significance of TMEM45A expression in the immune microenvironment of GC. These results provide theoretical support for assessing the role of TMEM45A in tumor immunity and its application as a biomarker for GC. We also demonstrated that TMEM45A can promote the progression of gastric cancer and inhibit the apoptosis of gastric cancer cells. We also obtained genes co-expressed with TMEM45A by co-expression method and performed functional analysis. We found that TMEM45A can activate the Wnt signaling pathway. We also used immunoregulatory molecules associated with TMEM45A to construct prognostic models. Firstly, three genes were screened from 30 immunomodulator molecules to establish a prediction model, and the risk value of each patient was measured using a risk-scoring formula, and GC patients were assigned to low- and high-risk groups based on the average risk score of the patients. Second, the survival curve of GC patients showed that the survival rate of GC patients in high-risk group was low. The risk curve and scatter plot demonstrated that the mortality of high-risk patients was remarkably higher than that of low-risk patients. The AUC value of the risk-scoring model was 0.747, indicating that the prognostic models could predict the prognosis of GC patients.

Although there are some limitations, this study provides us with a better understanding of the relationship between TMEM45A and GC. First of all, the data collected in this paper are almost from the online database. Second, the roles of TMEM45A gene in the diagnosis and treatment of GC have not been explored. Therefore, future studies are needed to further determine whether TMEM45A can be an effective therapeutic target or diagnostic marker. We did not discuss the detailed molecular mechanism of TMEM45A gene in GC. Hence, the exact mechanism of the relationship between TMEM45A gene and GC needs to be further explored.

5. Conclusion

In summary, by pan-cancer analysis, we found that TMEM45A is a carcinogen and a prognostic marker. The correlation between TMEM45A gene and GC was systematically analyzed. The expression of TMEM45A was upregulated in GC, and patients with TMEM45A overexpression had a poor prognosis. The relationships among TMEM45A, immune cell infiltration and immunomodulatory molecules were also explored. The findings demonstrated that TMEM45A could affect the infiltration of various immune cells. Therefore, TMEM45A may become a new cancer biomarker and therapeutic target for GC patients.

Conflict of Interests

The author has no conflicts with any step of the article preparation.

Consent for publications

The author read and approved the final manuscript for publication.

Ethical statement

Human specimens and animals were not used in this study.

Informed Consent

The authors declare that no patients were used in this study.

Data availability statement

The expression data of 33 cancer patients and the clinical data for survival analysis were derived from the TCGA database (https://cancergenome.nih.gov/). The gastric cancer patient database I used was derived from the GEO database (https://www.ncbi.nlm.nih.gov/geo/). I used gastric cancer cell line data from CCLE database (https://portals.broadinstitute.org/ccle). TCGA, GEO and CCLE are all open databases that are free for researchers to use, and each researcher can use the data in their own research projects.

Author contribution statement

Xie Qixin's main contributions are data collection, software download, data visualization, experimental validation, article writing and article revision. The major contributions of Tao Guo, Hon Deng and Changjun Yu are article revisions. Fang Changyi's main contribution is article revision and financial support.

Grant statement

Thanks to Dr. Changyi Fang for the support of the 2021-2022 National Natural Science Project (Fund number: 81902451).

References

1. Bray F, Laversanne M, Weiderpass E, Soerjomataram I (2021) The ever-increasing importance of cancer as a leading cause of premature death worldwide. Cancer-Am Cancer Soc 127:3029-3030. doi: 10.1002/cncr.33587
2. Sung H, Ferlay J, Siegel RL, Laversanne M, Soerjomataram I,

Jemal A et al (2021) Global Cancer Statistics 2020: GLOBOCAN Estimates of Incidence and Mortality Worldwide for 36 Cancers in 185 Countries. Ca-Cancer J Clin 71:209-249. doi: 10.3322/caac.21660
3. Thrift AP, El-Serag HB (2020) Burden of Gastric Cancer. Clin Gastroenterol H 18:534-542. doi: 10.1016/j.cgh.2019.07.045
4. Yusefi AR, Bagheri LK, Bastani P, Radinmanesh M, Kavosi Z (2018) Risk Factors for Gastric Cancer: A Systematic Review. Asian Pac J Cancer Prev 19:591-603. doi: 10.22034/APJCP.2018.19.3.591
5. Smyth EC, Nilsson M, Grabsch HI, van Grieken NC, Lordick F (2020) Gastric cancer. Lancet 396:635-648. doi: 10.1016/S0140-6736(20)31288-5
6. Shah D, Bentrem D (2022) Environmental and genetic risk factors for gastric cancer. J Surg Oncol 125:1096-1103. doi: 10.1002/jso.26869
7. Hwang H, Dwyer J, Russell RM (1994) Diet, Helicobacter pylori infection, food preservation and gastric cancer risk: are there new roles for preventative factors? Nutr Rev 52:75-83. doi: 10.1111/j.1753-4887.1994.tb01394.x
8. Lao-Sirieix P, Caldas C, Fitzgerald RC (2010) Genetic predisposition to gastro-oesophageal cancer. Curr Opin Genet Dev 20:210-217. doi: 10.1016/j.gde.2010.03.002
9. Usui Y, Taniyama Y, Endo M, Koyanagi YN, Kasugai Y, Oze I et al (2023) Helicobacter pylori, Homologous-Recombination Genes, and Gastric Cancer. New Engl J Med 388:1181-1190. doi: 10.1056/NEJMoa2211807
10. Hamashima C, Ogoshi K, Narisawa R, Kishi T, Kato T, Fujita K et al (2015) Impact of endoscopic screening on mortality reduction from gastric cancer. World J Gastroentero 21:2460-2466. doi: 10.3748/wjg.v21.i8.2460
11. Hamashima C (2014) Current issues and future perspectives of gastric cancer screening. World J Gastroentero 20:13767-13774. doi: 10.3748/wjg.v20.i38.13767
12. Lin JT (2014) Screening of gastric cancer: who, when, and how. Clin Gastroenterol H 12:135-138. doi: 10.1016/j.cgh.2013.09.064
13. Wang P, Zhao W, Sun J, Tao T, Chen X, Zheng YY et al (2018) Inflammatory mediators mediate airway smooth muscle contraction through a G protein-coupled receptor-transmembrane protein 16A-voltage-dependent Ca(2+) channel axis and contribute to bronchial hyperresponsiveness in asthma. J Allergy Clin Immun 141:1259-1268. doi: 10.1016/j.jaci.2017.05.053
14. Pedemonte N, Galietta LJ (2014) Structure and function of TMEM16 proteins (anoctamins). Physiol Rev 94:419-459. doi: 10.1152/physrev.00039.2011
15. Okuyama K, Yanamoto S (2022) TMEM16A as a potential treatment target for head and neck cancer. J Exp Clin Canc Res 41:196. doi: 10.1186/s13046-022-02405-2
16. Chen J, Wang D, Chen H, Gu J, Jiang X, Han F et al (2023) TMEM196 inhibits lung cancer metastasis by regulating the Wnt/beta-catenin signaling pathway. J Cancer Res Clin 149:653-667. doi: 10.1007/s00432-022-04363-w
17. Escobar A, Styrpejko DJ, Ali S, Cuajungco MP (2022) Transmembrane 163 (TMEM163) protein interacts with specific mammalian SLC30 zinc efflux transporter family members. Biochem Biophys Rep 32:101362. doi: 10.1016/j.bbrep.2022.101362
18. Styrpejko DJ, Cuajungco MP (2021) Transmembrane 163 (TMEM163) Protein: A New Member of the Zinc Efflux Transporter Family. Biomedicines 9:220. doi: 10.3390/biomedicines9020220
19. Sanchez VB, Ali S, Escobar A, Cuajungco MP (2019) Transmembrane 163 (TMEM163) protein effluxes zinc. Arch Biochem Biophys 677:108166. doi: 10.1016/j.abb.2019.108166
20. Hu M, Li P, Wang C, Feng X, Geng Q, Chen W et al (2022) Parkinson's disease-risk protein TMEM175 is a proton-activated proton channel in lysosomes. Cell 185:2292-2308. doi: 10.1016/j.cell.2022.05.021
21. Schmit K, Chen JW, Ayama-Canden S, Fransolet M, Finet L, Demazy C et al (2019) Characterization of the role of TMEM45A in cancer cell sensitivity to cisplatin. Cell Death Dis 10:919. doi: 10.1038/s41419-019-2088-x
22. Liu Y, Liu L, Mou ZX (2022) TMEM45A Affects Proliferation, Apoptosis, Epithelial-Mesenchymal Transition, Migration, Invasion and Cisplatin Resistance of HPV-Positive Cervical Cancer Cell Lines. Biochem Genet 60:173-190. doi: 10.1007/s10528-021-10094-3
23. Hayez A, Malaisse J, Roegiers E, Reynier M, Renard C, Haftek M et al (2014) High TMEM45A expression is correlated to epidermal keratinization. Exp Dermatol 23:339-344. doi: 10.1111/exd.12403
24. Wrzesinski T, Szelag M, Cieslikowski WA, Ida A, Giles R, Zodro E et al (2015) Expression of pre-selected TMEMs with predicted ER localization as potential classifiers of ccRCC tumors. Bmc Cancer 15:518. doi: 10.1186/s12885-015-1530-4
25. Weiner C, Hecht I, Kotlyar A, Shoshany N, Zadok D, Elbaz U et al (2021) Association of Variants in TMEM45A With Keratoglobus. Jama Ophthalmol 139:1089-1095. doi: 10.1001/jamaophthalmol.2021.3172
26. Guo J, Chen L, Luo N, Yang W, Qu X, Cheng Z (2015) Inhibition of TMEM45A suppresses proliferation, induces cell cycle arrest and reduces cell invasion in human ovarian cancer cells. Oncol Rep 33:3124-3130. doi: 10.3892/or.2015.3902
27. Jiang H, Chen H, Wan P, Liang M, Chen N (2021) Upregulation of TMEM45A Promoted the Progression of Clear Cell Renal Cell Carcinoma in vitro. J Inflamm Res 14:6421-6430. doi: 10.2147/JIR.S341596
28. Li T, Fu J, Zeng Z, Cohen D, Li J, Chen Q et al (2020) TIMER2.0 for analysis of tumor-infiltrating immune cells. Nucleic Acids Res 48:W509-W514. doi: 10.1093/nar/gkaa407
29. Li T, Fan J, Wang B, Traugh N, Chen Q, Liu JS et al (2017) TIMER: A Web Server for Comprehensive Analysis of Tumor-Infiltrating Immune Cells. Cancer Res 77:e108-e110. doi: 10.1158/0008-5472.CAN-17-0307
30. Ru B, Wong CN, Tong Y, Zhong JY, Zhong S, Wu WC et al (2019) TISIDB: an integrated repository portal for tumor-immune system interactions. Bioinformatics 35:4200-4202. doi: 10.1093/bioinformatics/btz210
31. Thorsson V, Gibbs DL, Brown SD, Wolf D, Bortone DS, Ou YT et al (2018) The Immune Landscape of Cancer. Immunity 48:812-830. doi: 10.1016/j.immuni.2018.03.023
32. Tao Z, Wang S, Wu C, Wu T, Zhao X, Ning W et al (2023) The repertoire of copy number alteration signatures in human cancer. Brief Bioinform 24doi: 10.1093/bib/bbad053
33. Zeng D, Li M, Zhou R, Zhang J, Sun H, Shi M et al (2019) Tumor Microenvironment Characterization in Gastric Cancer Identifies Prognostic and Immunotherapeutically Relevant Gene Signatures. Cancer Immunol Res 7:737-750. doi: 10.1158/2326-6066.CIR-18-0436
34. Bray F, Ferlay J, Soerjomataram I, Siegel RL, Torre LA, Jemal A (2018) Global cancer statistics 2018: GLOBOCAN estimates of incidence and mortality worldwide for 36 cancers in 185 countries. Ca-Cancer J Clin 68:394-424. doi: 10.3322/caac.21492
35. Rashkin SR, Graff RE, Kachuri L, Thai KK, Alexeeff SE, Blatchins MA et al (2020) Pan-cancer study detects genetic risk variants and shared genetic basis in two large cohorts. Nat Commun 11:4423. doi: 10.1038/s41467-020-18246-6
36. Liu X, Wu J, Zhang D, Bing Z, Tian J, Ni M et al (2018) Identification of Potential Key Genes Associated With the Pathogenesis

and Prognosis of Gastric Cancer Based on Integrated Bioinformatics Analysis. Front Genet 9:265. doi: 10.3389/fgene.2018.00265

37. Li L, Ouyang Y, Wang W, Hou D, Zhu Y (2019) The landscape and prognostic value of tumor-infiltrating immune cells in gastric cancer. Peerj 7:e7993. doi: 10.7717/peerj.7993
38. Noh SH, Park SR, Yang HK, Chung HC, Chung IJ, Kim SW et al (2014) Adjuvant capecitabine plus oxaliplatin for gastric cancer after D2 gastrectomy (CLASSIC): 5-year follow-up of an open-label, randomised phase 3 trial. Lancet Oncol 15:1389-1396. doi: 10.1016/S1470-2045(14)70473-5
39. Sano T, Coit DG, Kim HH, Roviello F, Kassab P, Wittekind C et al (2017) Proposal of a new stage grouping of gastric cancer for TNM classification: International Gastric Cancer Association staging project. Gastric Cancer 20:217-225. doi: 10.1007/s10120-016-0601-9
40. Li Y, Cheng X, Yan J, Jiang S (2022) CTHRC1 facilitates bladder cancer cell proliferation and invasion through regulating the PI3K/Akt signaling pathway. Arch Med Sci 18:183-194. doi: 10.5114/aoms.2019.85718
41. Costa AC, Santos J, Gil DCR, Medeiros R (2021) Impact of immune cells on the hallmarks of cancer: A literature review. Crit Rev Oncol Hemat 168:103541. doi: 10.1016/j.critrevonc.2021.103541
42. Li W, Li M, Wang H, Peng Y, Dong S, Lu Y et al (2021) Infiltrating Immune Cells in Gastric Cancer: A Novel Predicting Model for Prognosis. J Cancer 12:965-975. doi: 10.7150/jca.51079
43. Yang Y, He W, Wang ZR, Wang YJ, Li LL, Lu JZ et al (2021) Immune Cell Landscape in Gastric Cancer. Biomed Res Int 2021:1930706. doi: 10.1155/2021/1930706
44. Liu Y, Xie S, Zhu K, Guan X, Guo L, Lu R (2021) CALD1 is a prognostic biomarker and correlated with immune infiltrates in gastric cancers. Heliyon 7:e07257. doi: 10.1016/j.heliyon.2021.e07257
45. Zeng Q, Li L, Feng Z, Luo L, Xiong J, Jie Z et al (2021) LCP1 is a prognostic biomarker correlated with immune infiltrates in gastric cancer. Cancer Biomark 30:105-125. doi: 10.3233/CBM-200006